

See discussions, stats, and author profiles for this publication at: <https://www.researchgate.net/publication/21745290>

# Three-dimensional structure of the quinoprotein methylamine dehydrogenase from *Paracoccus denitrificans* determined by molecular replacement at 2.8 Å resolution

ARTICLE in PROTEINS STRUCTURE FUNCTION AND BIOINFORMATICS · OCTOBER 1992

Impact Factor: 2.63 · DOI: 10.1002/prot.340140214 · Source: PubMed

---

CITATIONS

47

---

READS

18

6 AUTHORS, INCLUDING:



**Francis Scott Mathews**

Washington University in St. Louis

192 PUBLICATIONS 14,725 CITATIONS

SEE PROFILE



**Victor L Davidson**

University of Central Florida

219 PUBLICATIONS 5,290 CITATIONS

SEE PROFILE



**Frederic Vellieux**

Academy of Sciences of the Czech Republic

68 PUBLICATIONS 1,266 CITATIONS

SEE PROFILE

# Three-Dimensional Structure of the Quinoprotein Methylamine Dehydrogenase From *Paracoccus denitrificans* Determined by Molecular Replacement at 2.8 Å Resolution

Longyin Chen,<sup>1</sup> F. Scott Mathews,<sup>1</sup> Victor L. Davidson,<sup>2</sup> Eric G. Huizinga,<sup>3</sup> Frederic M.D. Vellieux,<sup>3</sup> and Wim G.J. Hol<sup>3</sup>

<sup>1</sup>Department of Cell Biology and Physiology, Washington University School of Medicine, St. Louis, Missouri 63110,

<sup>2</sup>Department of Biochemistry, the University of Mississippi Medical Center, Jackson, Mississippi 39216, and

<sup>3</sup>BIOSON Research Institute, University of Groningen, 9747 AG Groningen, The Netherlands

**ABSTRACT** The three-dimensional structure of the quinoprotein methylamine dehydrogenase from *Paracoccus denitrificans* (PD-MADH) has been determined at 2.8 Å resolution by the molecular replacement method combined with map averaging procedures, using data collected from an area detector. The structure of methylamine dehydrogenase from *Thiobacillus versutus*, which contains an "X-ray" sequence, was used as the starting search model. MADH consists of 2 heavy (H) and 2 light (L) subunits related by a molecular 2-fold axis. The H subunit is folded into seven four-stranded  $\beta$  segments, forming a disk-shaped structure, arranged with pseudo-7-fold symmetry. A 31-residue elongated tail exists at the N-terminus of the H subunit in MADH from *T. versutus* but is partially digested in this crystal form of MADH from *P. denitrificans*, leaving the H subunit about 18 residues shorter. Each L subunit contains 127 residues arranged into 10  $\beta$ -strands connected by turns. The active site of the enzyme is located in the L subunit and is accessible via a hydrophobic channel between the H and L subunits. The redox cofactor of MADH, tryptophan tryptophylquinone is highly unusual. It is formed from two covalently linked tryptophan side chains at positions 57 and 107 of the L subunit, one of which contains an orthoquinone.

© 1992 Wiley-Liss, Inc.

**Key words:** amino acid-derived cofactor, crystal structure, methylamine dehydrogenase, molecular replacement, oxidoreductase, *Paracoccus denitrificans*, pyrroloquinoline quinone, quinoprotein, tryptophan tryptophylquinone

## INTRODUCTION

When certain methylotrophic bacteria (for review, see ref. 1) are grown in a medium in which meth-

ylamine is the sole source of carbon and energy, an enzyme, methylamine dehydrogenase (MADH, EC 1.4.99.3) is induced.<sup>2</sup> The enzyme catalyzes the oxidation of primary amines into the corresponding aldehyde and transfers electrons to c-type cytochromes through a mediating blue copper protein, amicyanin.<sup>3</sup> Methylamine dehydrogenase from *Paracoccus denitrificans* (PD-MADH<sup>4</sup>) is a tetramer of two different subunits, H<sub>2</sub>L<sub>2</sub>, with molecular weight 46,700 for the heavy (H) subunits and 15,500 for the light (L) subunits giving a total molecular weight of 124,000.

MADH belongs to the quinoprotein family of enzymes which contains various quinonoid redox cofactors. Other quinoproteins include bacterial methanol and glucose dehydrogenase,<sup>5,6</sup> which contain the noncovalently bound cofactor pyrroloquinoline quinone (PQQ,<sup>7</sup> see Fig. 1a) and mammalian serum amine oxidase<sup>8</sup> which contains covalently bound trishydroxy phenylalanine (TOPA, Fig. 1b). MADH has recently been shown to contain a novel and unique prosthetic group as its redox cofactor, a double tryptophan quinone<sup>9</sup> formed by two covalently linked tryptophan side chains, one of which has been modified to contain an ortho quinone. The proposed structure of this cofactor, named tryptophan tryptophylquinone (TTQ), is shown in Figure 1c.

The complete amino acid sequence of MADH from any source has not yet been reported, although that

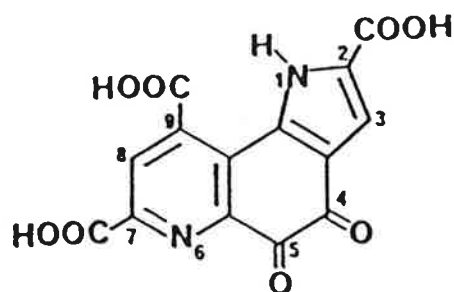
Received August 23, 1991; revision accepted February 3, 1992.

Address reprint requests to F. Scott Mathews, Department of Cell Biology and Physiology, Box 8225, Washington University School of Medicine, St. Louis, MO 63110.

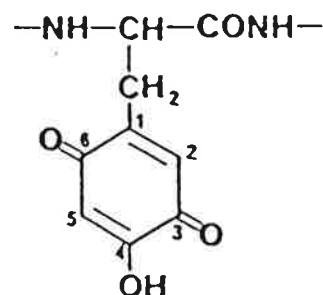
Current address of Frederic M.D. Vellieux: Laboratoire d'Ingénierie des Protéines, Centre d'Etudes Nucleaires, Grenoble, 85X Centre de Tri, 38041 Grenoble, Cedex, France.

Abbreviations: AM1, *Methylobacterium extoquens* AM1; FFT, fast Fourier transform; HT, hydroxytryptamine; MADH, methylamine dehydrogenase; MIR, multiple isomorphous replacement; PD, *Paracoccus denitrificans*; PQQ, pyrroloquinoline quinone; R-factor,  $\sum |F_{\text{obs}} - F_{\text{calc}}| / \sum |F_{\text{obs}}|$ ; SIR, single isomorphous replacement; TTQ, tryptophan tryptophylquinone; TV, *Thiobacillus versutus*.

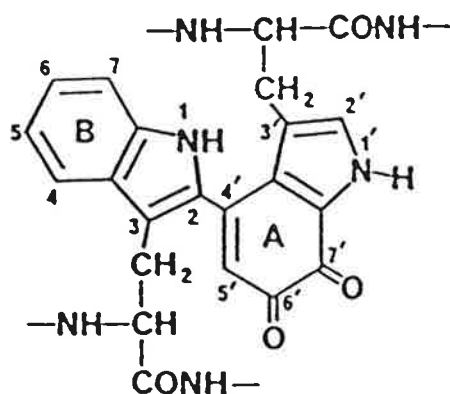
© 1992 WILEY-LISS, INC.



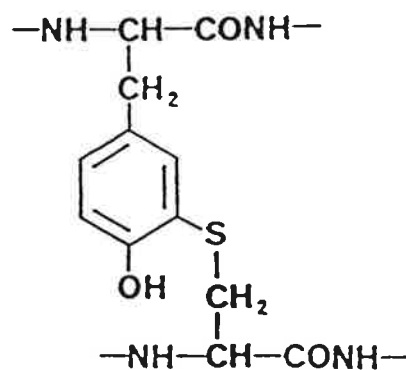
a



b



c



d

Fig. 1. Novel redox cofactors: (a) pyrroloquinoline quinone (PPQ<sup>7</sup>), (b) trishydroxy phenylalanine (6-hydroxydopaquinone, TOPA<sup>8</sup>), (c) tryptophan tryptophylquinone (TTQ<sup>9</sup>), (d) cross-linked tyrosine-cysteine in galactose oxidase.<sup>38</sup>

of several fragments from a variety of sources have been determined by sequencing either the protein or the gene. The chemical<sup>10</sup> and DNA<sup>11</sup> sequences of the L subunit of MADH from *Methylobacterium extorquens* AM1 (AM1-MADH), formerly called *Pseudomonas* AM1, have been determined. More recently, a partial gene sequence of PD-MADH, consisting of the last 31 residues of the L subunit, was reported.<sup>12</sup>

The three-dimensional structure of MADH from *Thiobacillus versutus* (TV-MADH) has been deter-

mined.<sup>13,14</sup> This model contains an amino acid sequence derived from the electron density distribution. A preliminary crystallographic study of PD-MADH and of an intermolecular complex between PD-MADH and amicyanin has been reported.<sup>15</sup> An analysis of the electron density maps of both TV-MADH and PD-MADH corresponding to the cofactor-containing region has appeared recently<sup>16</sup> in which direct evidence in support of the proposed structure<sup>9</sup> of the TTQ cofactor (Fig. 1c) was presented. In the present paper we fully describe the

TABLE I. Data Collection Statistics

Dataset	Cell parameters			No. of reflections (collected/possible)	$d_{\min}$ (Å)	$R_{\text{sym}}^*$	$\Delta F_{\text{iso}}^\dagger$
	$a$	$b$	$c$				
Native	152.19	135.50	54.89	25417/29936	2.76	5.62	
UO <sub>2</sub> (NO <sub>3</sub> ) <sub>2</sub> derivative							
Crystal 1	151.14	135.24	54.85	27295/30487	2.74	5.08	10.9
Crystal 2	151.67	135.12	55.37	13020/31801	2.71	9.22	14.6
Crystal 3		(Not refined)		25414/32311	2.70	8.42	15.6
Crystal 4		(Not refined)		19932/32273	2.70	5.84	13.2
Correlation $R_{\text{sym}}$ , 4 crystals <sup>‡</sup>						8.9	
K <sub>3</sub> (UO) <sub>2</sub> F <sub>5</sub> derivative							
Crystal 1	151.51	134.97	54.68	26030/30511	2.74	5.32	12.8
Crystal 2	151.59	135.10	54.92	26271/30795	2.71	5.82	12.4
Correlation $R_{\text{sym}}$ , 2 crystals <sup>‡</sup>						7.0	
K <sub>2</sub> PtCl <sub>4</sub> derivative							
Crystal 1	150.75	135.98	55.24	29666/35762	2.62	9.91	20.1
Crystal 2	150.28	135.10	54.70	21706/30793	2.72	9.18	21.7
Correlation $R_{\text{sym}}$ , 2 crystals <sup>‡</sup>						13.8	

\* $R_{\text{sym}} = \sum |I_{\text{obs}} - I_{\text{avg}}| / \sum I_{\text{obs}}$ .

<sup>†</sup> $\Delta F_{\text{iso}}$  is the mean isomorphous structure factor difference.

<sup>‡</sup>The individual data sets for each derivative were merged using the ROCKS program.<sup>18</sup>

crystal structure analysis of PD-MADH at 2.8 Å resolution on which in part the previous paper was based.

## EXPERIMENTAL PROCEDURES

The crystallization of PD-MADH was described previously.<sup>15</sup> However, in order to grow suitable crystals of PD-MADH, we found it necessary to incubate the protein at room temperature (23–24°C) for about 3 weeks in 5 mM phosphate buffer (NaH<sub>2</sub>PO<sub>4</sub>:K<sub>2</sub>HPO<sub>4</sub> = 90:10); otherwise the protein usually precipitates or produces poor quality crystals. Afterward crystals are grown by the hanging-drop vapor diffusion method using 2.3–2.4 M unbuffered ammonium sulfate as precipitant. In this way chunky crystals with a yellow-green color and dimensions of about 1 × 0.8 × 0.2 mm can be obtained. The crystals exhibit space group  $P2_12_12_1$  with unit cell parameters  $a = 152.19$  Å,  $b = 135.51$  Å, and  $c = 54.89$  Å, and contain one molecule per asymmetric unit.<sup>15</sup> They diffract beyond 2.5 Å resolution.

Initially an attempt was made to solve the structure of PD-MADH by the MIR method using 3 types of heavy atom derivatives, UO<sub>2</sub>(NO<sub>3</sub>)<sub>2</sub>, K<sub>2</sub>PtCl<sub>4</sub>, and K<sub>3</sub>(UO)<sub>2</sub>F<sub>5</sub> (Table I). X-Ray diffraction data were collected at the Argonne National Laboratory using a Nicolet area detector mounted on an Elliot GX20 rotating anode X-ray generator and processed using the XENGEN data reduction system.<sup>17</sup> All of the data were collected at room temperature. A complete data set could be collected from one native crystal but collection of the derivative data involved recording anomalous scattering data and required 2–4 crystals for each derivative. The derivative data sets were locally scaled to and correlated with the native data using the ROCKS crystallographic com-

puting program<sup>18</sup> as adapted for the VAX computer.<sup>19</sup> Table I summarizes the data collection results.

Two binding sites each were obtained for the UO<sub>2</sub>(NO<sub>3</sub>)<sub>2</sub> and K<sub>3</sub>(UO)<sub>2</sub>F<sub>5</sub> derivatives by inspection of the isomorphous difference Patterson maps. Two additional minor sites for the UO<sub>2</sub>(NO<sub>3</sub>)<sub>2</sub> derivative were obtained using the difference Patterson superposition search program HASSP.<sup>20</sup> Eight binding sites were obtained for the K<sub>2</sub>PtCl<sub>4</sub> derivative in a cross difference Fourier map using phases calculated by SIR from the UO<sub>2</sub>(NO<sub>3</sub>)<sub>2</sub> sites. The heavy atom binding sites for all 3 derivatives were refined at 3.0 Å resolution by least squares using the heavy atom parameter refinement program, HEAVY.<sup>21</sup>

MIR phases of the protein were computed at 3.0 Å resolution based on the refined heavy atom parameters. The resulting electron density map could not be interpreted, even to define the molecular boundary. Solvent flattening<sup>22</sup> was carried out in order to improve the protein phases, but the resulting electron density map was still not clear enough to trace the polypeptide chain. An unsuccessful attempt was made to locate the orientation of the molecular 2-fold axis using the self-rotation function.<sup>23</sup> The positions of the heavy atoms were also plotted on the electron density map and examined carefully in an attempt to locate the molecular diad axis, but this approach was also unsuccessful. Consequently, it was not possible to average the electron density about the 2-fold axis to improve the map.

At this stage, the coordinates of MADH from *Thiobacillus versutus* (TV-MADH), which contains a preliminary sequence derived from the electron density map, became available.<sup>13,14</sup> We decided to apply the molecular replacement method<sup>24</sup> to solve the

TABLE II. Molecular Replacement Results of MADH

Program	Peak rank	Maximum* or <i>R</i> -factor <sup>†</sup> (%)	$\alpha$	$\beta$	$\gamma$	$X_c^{\ddagger}$	$Y_c^{\ddagger}$	$Z_c^{\ddagger}$	Comments
CROSUM <sup>§</sup>	1	100.00	90.00	40.00	20.00	—	—	—	Global coarse grid search
	2	96.52	95.00	85.00	10.00	—	—	—	
	3	80.52	75.00	50.00	205.00	—	—	—	
	4	80.04	47.50	15.00	245.00	—	—	—	
CROSUM	1	100.00	90.00	38.00	20.00	—	—	—	Local fine grid search
	2	100.00	95.00	83.00	10.00	—	—	—	
LATSUM**	1	100.00	91.00	39.00	18.00	—	—	—	Local fine grid search
	2	100.00	94.00	82.00	12.00	—	—	—	
TRNSUM <sup>††</sup>	—	—	—	—	—	0.3950	0.1500	—	Molecule 2 to 1
	—	—	—	—	—	—	0.1500	0.3300	Molecule 3 to 1
	—	—	—	—	—	0.3950	—	0.3275	Molecule 4 to 1
RVAMAP <sup>‡‡</sup>	1	0.530	—	—	—	0.3900	0.1500	0.3300	Global coarse grid search
	2	0.589	—	—	—	0.1800	0.1500	0.3300	
	3	0.590	—	—	—	0.2700	0.1500	0.3300	
RVAMAP	1	0.472	—	—	—	0.4000	0.1500	0.3300	Local fine grid search
RMINIM <sup>§§</sup>	—	0.395	91.35	38.45	17.65	0.396	0.1500	0.3285	

\*Percentage of the maximum peak height in the programs CROSUM and LATSUM.

<sup>†</sup>*R*-factor found by programs RVAMAP and RMINIM.

<sup>‡</sup> $X$ ,  $Y$ , and  $Z$  are the fractional coordinates of the search model in the PD-MADH unit cell.

<sup>§</sup>Crowther rotation function.<sup>26</sup> In the coarse grid search, the increments in  $\alpha$ ,  $\beta$ , and  $\gamma$  were 2.5°, 2°, and 5°, respectively. In the fine grid search the increment in  $\beta$  was 1°.

<sup>\*\*</sup>Lattman rotation function.<sup>27</sup> The increments in the Eulerian angles were 1°. The search was carried out in a small region around the peak positions found in CROSUM.

<sup>††</sup>Crowther–Blow translation function.<sup>28</sup>

<sup>‡‡</sup>*R*-factor search program<sup>25</sup> for optimal translation vector of search molecule in unknown cell. In the global coarse grid search, increments of 0.002 were used and in the local fine grid search increments of 0.001 were used.

<sup>§§</sup>Rigid body *R*-factor minimization program.<sup>25,29</sup>

structure of PD-MADH using TV-MADH as a starting model and employing the program package MERLOT.<sup>25</sup> A resolution range of 4–8 Å was used throughout, except for certain subprograms which require a slightly higher resolution limit. The full tetramer of TV-MADH was used as the search model and an artificial triclinic unit cell of 185 × 185 × 185 Å<sup>3</sup> was used for the structure factor calculation. The integration radius used was 23.9 Å.

A cross rotation function using Crowther's procedure<sup>26</sup> was calculated first on a coarse grid (Table II). The two highest peaks were of nearly equal magnitude and the third highest peak was about 80% of the highest. The two top peaks were refined first using a fine grid search by the same procedure and then by a fine grid search using the Lattman rotation function<sup>27</sup> (Table II). The two major peaks found in the rotation function represent two orientations of the search model which differ by 180° rotation about the molecular 2-fold axis and are thus equivalent, demonstrating that the unknown structure does possess a noncrystallographic diad as expected.

Using the three Euler angles obtained from the rotation function solution, the Crowther–Blow translation function was calculated.<sup>28</sup> This produced

a single major peak for each of the three intermolecular vectors between molecules related by the symmetry elements in space group  $P2_12_12_1$ . Analysis of these peaks showed that the translation parameters for the center of the molecule ( $X_c$ ,  $Y_c$ , and  $Z_c$ , Table II) were consistent with each other according to this space group symmetry. A three-dimensional search for a minimum *R*-factor was also carried out to verify the results from the translation function.<sup>25</sup> The results are in good agreement with each other. At this point a rigid body *R*-factor minimization was carried out<sup>25,29</sup> in which the orientation and translation parameters were alternatively adjusted. After 20 cycles of refinement an *R*-factor of 0.395 was obtained.

Refinement of the PD-MADH structure was carried out using the molecular dynamics program GROMOS modified to include crystallographic restraints.<sup>30,31</sup> This was followed by additional least squares refinement by the Hendrickson–Konnert procedure<sup>32</sup> using the program PROFFT.<sup>33</sup> No manual refitting was done since the true amino acid sequence of neither PD-MADH nor TV-MADH was known. The molecular dynamics refinement consisted of an initial 200 steps of energy minimization followed by 550 steps of restrained molecular dy-

TABLE III. Refinement Results of MADH by GROMOS/PROLSQ

Run	Resolution limits (Å)	Number of steps	$\sigma_x$	Rms deviation ( $ F_o  -  F_c $ )		R-factor (%)	
				Start	End	Start	End
EMX 1	3.5–8.0	200	8.5	9.9	9.3	37.7	32.5
MDX 1	3.5–8.0	100	8.0	9.3	9.1	32.5	31.9
MDX 2	3.2–8.0	200	7.0	9.7	8.3	35.5	30.5
MDX 3	2.8–6.0	100	7.0	8.3	7.9	34.4	32.2
MDX 4	2.8–6.0	50	7.0	7.9	7.8	32.2	31.9
MDX 5	2.8–6.0	100	6.5	7.8	7.7	31.6	30.4
EMX 2	2.8–6.0	100	6.0	7.7	7.2	30.4	28.6

PROLSQ Results					
Number of cycles	R-factors		Temperature factor	Mean B (Å <sup>2</sup> )	Resolution range (Å)
	Initial	Final			
3	0.293	0.271	Overall	9.38	6.0–2.8
6	0.271	0.246	Individual	7.84	6.0–2.8

\*Molecular dynamics refinement. EMX and MDX refer to energy minimization and molecular dynamics refinement with X-ray restraints, respectively.  $\sigma_x$  is used for the calculation of the weight ( $w_x = 1/\sigma_x^2$ ) of the X-ray energy:  $E_{x\text{-ray}} = w_x \sum (|F_{\text{obs}}| - |F_{\text{calc}}|)^2$ .

namics refinement at a temperature of 350 K. One step of molecular dynamics refinement corresponds to a 2-fsec time step. Finally 100 steps of energy minimization were performed. During this procedure all atomic temperature factors were kept at 12 Å<sup>2</sup>. The course of the refinement is given in Table III. The resultant *R*-factor at this stage was 0.285.

Restrained refinement was continued with PROLSQ so that temperature factors could be refined. This included 3 cycles of positional refinement with an overall temperature factor of 9.4 Å<sup>2</sup>, obtained from a Wilson plot followed by six cycles of combined positional and individual atomic temperature factor refinement. The final *R*-factor was 0.246. The statistics of the refined model from the final PROLSQ results are given in Table IV.

After refinement, the electron density map was averaged about the molecular 2-fold axis using Brice's procedures.<sup>34</sup> This was done in order to improve the electron density in the region of the prosthetic group which had not been included in the refinement. An averaged map may also remove bias from the starting model in areas where amino acid sequence differences occur.

## RESULTS AND DISCUSSION

### Tetrameric Structure

The molecule of MADH is a heterotetramer, consisting of 2 H and two L subunits related by a molecular two-fold axis (Fig. 2). The H<sub>2</sub>L<sub>2</sub> tetramer forms an approximate parallelepiped when projected along the molecular 2-fold axis, with dimensions 76 Å by 61 Å, as shown in Figure 2. In this orientation, the molecule is about 45 Å thick. Each H subunit interacts extensively with one L subunit and so the structure can best be described as a dimer of two

identical HL dimers. The "X-ray" sequence deduced from the TV-MADH electron density distribution<sup>13,14</sup> was used for 368 residues for each H subunit and 121 (7–127) residues for each L subunit. The basic molecular features of TV-MADH and PD-MADH are very similar judging by the unambiguous results of molecular replacement, the generally good fit of the TV structure to the PD map, and the relatively low *R*-factor resulting from the PD-MADH structure refinement based on an approximate amino acid sequence.

Within the tetrameric molecule, two heavy subunits H<sub>1</sub> and H<sub>2</sub> interact slightly with each other in the region close to the noncrystallographic 2-fold axis, while the two light subunits L<sub>1</sub> and L<sub>2</sub> are completely separated (Fig. 2). The H<sub>1</sub>–L<sub>2</sub> interactions are minimal, mainly involving contacts between the L subunit (see below) and the N-terminal extension of the H subunit. The latter forms a long arm, stretching to embrace the L subunit from the other HL group. The most extensive intramolecular interactions exist between the H<sub>1</sub> and L<sub>1</sub> subunits. Based on the "X-ray sequence" of TV-MADH, these interactions involve mainly nonpolar residues, some of which form a hydrophobic channel. The redox center, i.e., the TTQ cofactor of the enzyme is located in this region.

### The H Subunit and the Missing N-Terminal Extension

The H subunit can be divided into two sections as shown in Figure 3. The first section is a long N-terminal extension while the second, major section is a compact, disc-shaped structure with seven repeated fragments with very similar structural features. Each fragment is composed of a four-stranded

TABLE IV. Statistics of the Refined Model After PROLSQ

	Number	Rms deviation from ideality	Target variance
Stereochemistry			
Covalent bonds (Å)	7,086	0.017	0.020
Bond angles (°)	9,652	0.061	0.040
Planar distances (Å)	2,510	0.069	0.050
Least-squares planes (Å)	1,258	0.010	0.020
Peptide	978	0.009	
Aromatic	90	0.013	
Chiral center volume (Å <sup>2</sup> )	1,084	0.222	0.150
Single torsion contacts	2,033	0.230	0.500
Multiple torsion contacts	2,321	0.329	0.500
Possible H bond contacts	286	0.260	0.500
Planar torsion (°)	1,000	9.7	3.0
Staggered torsion (°)	1,016	24.6	15.0
Orthonormal torsion (°)	86	32.9	20.0
Thermal factor			
<i>B</i> for main chain bonds (Å <sup>2</sup> )	4,100	0.572	1.000
<i>B</i> for main chain angles (Å <sup>2</sup> )	5,214	0.955	1.500
<i>B</i> for side chain bonds (Å <sup>2</sup> )	2,986	0.967	1.000
<i>B</i> for side chain angles (Å <sup>2</sup> )	4,438	1.385	1.500
Total reflections	23,166		
Standard <i>R</i> -factor		0.246	

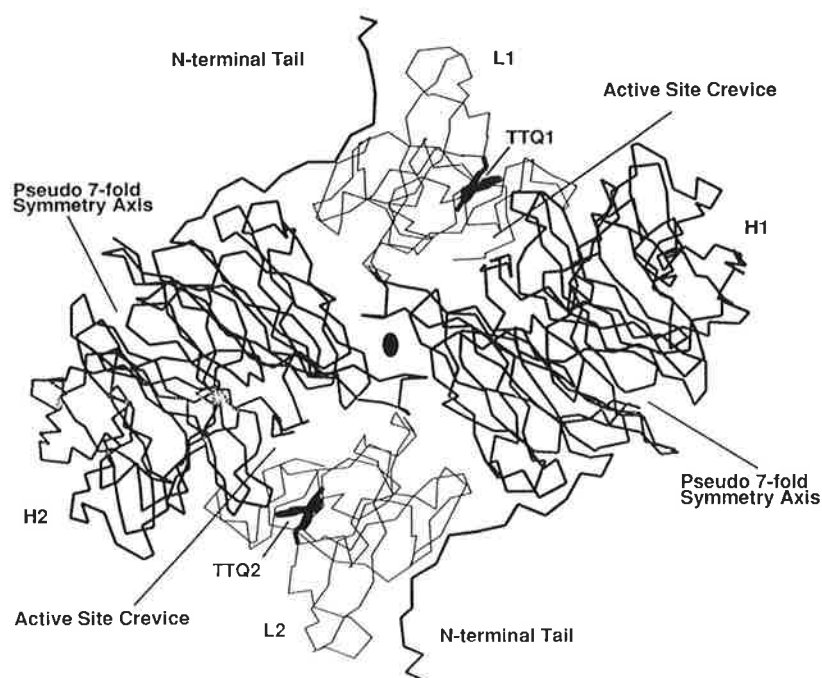


Fig. 2. The tetrameric structure of PD-MADH (backbone). The MADH tetramer can be described as a dimer of two identical HL dimers related by a molecular 2-fold axis as indicated in the figure. Within one tetramer, each H subunit (in thick lines) interacts with both L subunits (in thin lines). The active sites are located in the region of the H<sub>1</sub>-L<sub>1</sub> and H<sub>2</sub>-L<sub>2</sub> interface. The two TTQ redox cofactors in the H<sub>2</sub>L<sub>2</sub> tetramer are bound to the L subunits. The

pseudo-7-fold symmetry axis of the H subunits, which are approximately in the plane of the diagram, are indicated. The short tail at the N-terminus of each H subunit interacts with the L subunit of the other HL dimer. This N-terminus is in the crystal about 18 residues shorter than native PD-MADH and than in TV-MADH due to proteolysis as discussed in the text (see also Fig. 4).

antiparallel  $\beta$ -sheet connected in a simple up-down-up-down "W"-like leaflet structure. These leaflets are arranged around a central axis with pseudo-7-

fold symmetry (Fig. 3). In the MADH tetramer, these pseudo-7-fold axes lie in a plane approximately perpendicular to the molecular 2-fold axis

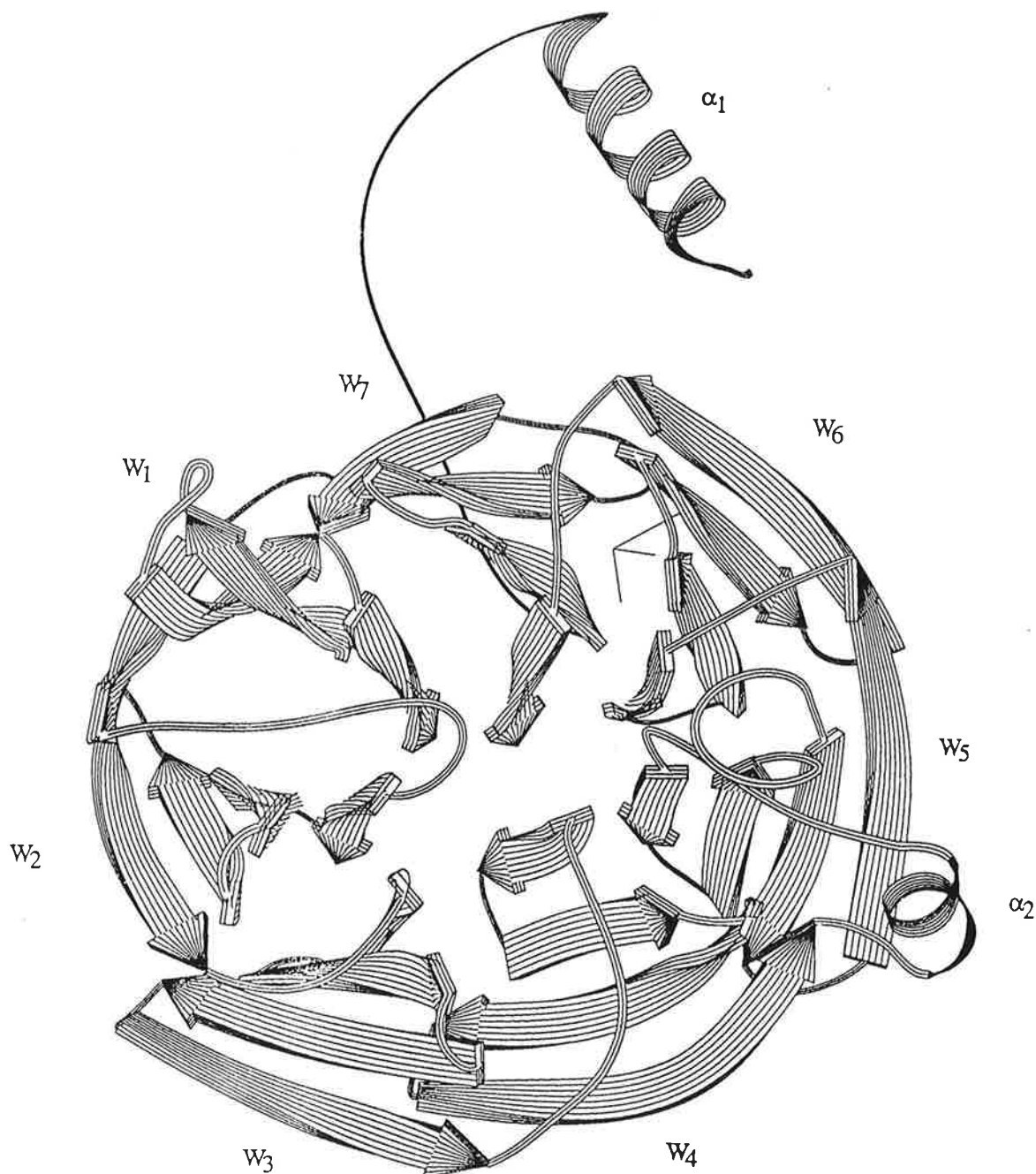


Fig. 3. The H subunit. The H subunit is a compact, disc-shaped domain containing seven repeated units in addition to an N-terminal extension. Each unit is composed of four antiparallel  $\beta$ -strands in a "W"-shape. The overall conformation of the disc shows pseudo-7-fold symmetry.

(Fig. 2). An additional short helix occurs in the connection between leaflets W4 and W5.

The most apparent difference between PD-MADH and TV-MADH in the crystalline state exists at the N-terminus. In the TV-MADH structure, the first 31 residues of the H subunit form a hairpin shaped extension which embraces the light subunit from another HL group (Fig. 2). The first 16 residues form

4.5 turns of  $\alpha$ -helix which is followed by a 3-residue reverse turn at positions 17–19. The remaining dozen residues adopt an extended conformation and return the chain to the main body of the H subunit. In the electron density map of PD-MADH, however, the  $\alpha$ -helical portion is almost entirely absent and only the segment from 19 to 31 is present, as shown in Figure 4. The results of least-squares refinement



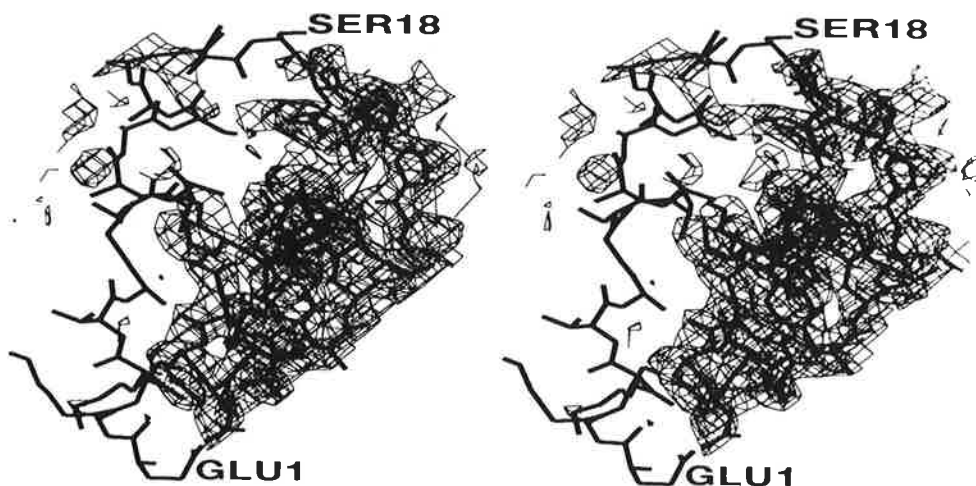


Fig. 4. The missing N-terminus of the H subunit. In the X-ray sequence of TV-MADH, the first 31 residues at the N-terminus form a hairpin extension which embraces the L subunit from the other HL dimer. The hairpin contains a turn from residues 17 to 19 and the segment before the turn forms an  $\alpha$ -helix. In the electron

density map of PD-MADH, however, the  $\alpha$ -helix portion is entirely missing. The electron density was calculated with coefficients ( $2F_o - F_c$ ) and phases obtained from the final cycle of least-squares refinement.

of the PD-MADH structure also indicated the absence of the helix since the temperature factors of the first 18 residues are considerably higher than those of the other residues. While the average temperature factor of the whole molecule is about  $8 \text{ \AA}^2$ , those of the first 18 residues are in general larger than  $40 \text{ \AA}^2$ . The most likely explanation for the absence of this 18-residue fragment is proteolytic degradation. Considering the procedure required to grow crystals of PD-MADH, hydrolysis could very well have occurred since the protein solution must stand for 3 weeks prior to crystallization.

In order to test the possibility of proteolysis, an SDS gel electrophoresis experiment was carried out on a PhastSystem to compare the aged protein samples with fresh ones. The results showed that the H subunit of the aged samples migrated as lighter bands. A mixture of fresh and aged samples migrated as two separate bands differing by approximately MW 2,000, at a mean position of  $M_r = 45,000$ , which is expected for the heavy subunit. This difference is consistent with earlier observation of degradation upon aging of the native enzyme and of the isolated H subunit to produce bands approximately MW 2,000 smaller than the fresh protein (V. L. Davidson, unpublished results). The clear absence of the N-terminal helix in the PD-MADH structure serves as evidence for minimal bias from the starting model in the molecular replacement procedure.

### The L Subunit Structure

The general structure of the L subunit of PD-MADH is very similar to that of TV-MADH. The L subunit comprises 121 residues, numbered 7–127, and is dominated by  $\beta$  structure, containing a total

of 10  $\beta$  strands. Six of them form a twisted, rather distorted antiparallel  $\beta$ -sheet (Fig. 5). The order of strands is 8, 3, 10, 7, 6, 9 from right to left as shown in Figure 5. Some of these strands are quite long, although only a few residues of each strand are involved in the hydrogen bonding network of the sheet. The sheet is somewhat curled so that the last strand ( $\beta_9$ ) lies somewhat above the third from last ( $\beta_7$ ). The TTQ cofactor is tucked into this fold (see below). There are also four shorter  $\beta$  strands forming two antiparallel  $\beta$ -hairpins. Strand 1 and 2 form one such hairpin, although only about 2 pairs of residues connect the strands. The other one is formed by strands 4 and 5 and is more regular. Both pairs of  $\beta$ -hairpins are located on the edge of the molecule and are not involved with the central 6-stranded sheet. The rest of the residues are found in loops or random coil.

There are a large number of covalent connections within the L subunit. A total of 12 cysteine residues, deduced from: (1) the amino acid composition of the *T. versutus* enzyme (F. Huitema, J.A. Duine, and J.J. Beintema, unpublished results); (2) analogy with the sequence of AM1-MADH;<sup>10,11</sup> and (3) the "X-ray sequence,"<sup>13</sup> form six disulfide bonds.<sup>13,14</sup> These intrasubunit cross-links may be important for stabilizing the subunit from heat denaturation.<sup>2</sup>

A partial chemical sequence (Table V) of the first 25 residues at the N-terminal end of the L subunit of PD-MADH has been determined. Comparison of this partial chemical sequence with the final electron density map indicates that, as in the case of the TV-MADH structure, the first 6 residues of the L subunit are disordered or absent. The chemically determined sequence shows about 84% identity (16 out of 19) with the X-ray sequence of TV-MADH and about

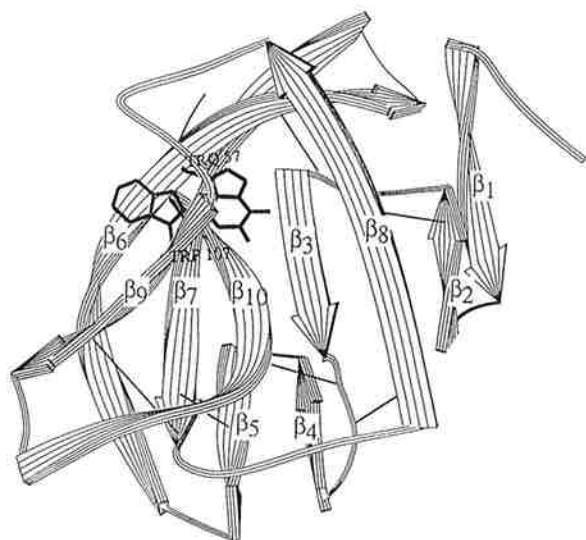


Fig. 5. The L subunit (ribbon model). The L subunit contains a total of 10  $\beta$ -strands. These form one six-strand sheet and two short two-strand sheets. The redox cofactor TTQ is located between three long anti-parallel strands  $\beta_6$ ,  $\beta_7$ , and  $\beta_9$ . A total of 12 cysteines (indicated by thin lines) form 6 disulfide bonds.

56% identity (14 out of 25) with the MADH from *M. extorquens* (AM1-MADH<sup>10,11</sup>).

A partial gene sequence of 31 residues at the C-terminal end of PD-MADH was reported recently,<sup>12</sup> which shows 97% amino acid sequence identity (30 out of 31) compared with that of AM1-MADH and about 65% identity (20 out of 31) with the TV-MADH X-ray sequence (Table V). The PD-MADH sequence has two insertions at positions 102 and 115 and two additional residues at the C-terminus compared with the X-ray sequence of TV-MADH.

We have tried to fit the new C-terminal sequence data for PD-MADH into the final  $2F_o - F_c$  electron density map from the refined structure. The apparent insertion of a phenylalanine at position 102 (Table V) is more easily accommodated in the map at position 99, which is an arginine in the AM1-MADH sequence (Fig. 6). The second insertion at position 115, an aspartic acid, is much more problematical and will require more extensive model building efforts which will only be possible when the full sequence of PD-MADH becomes available. The two additional residues at the C-terminus were also fitted into the density map. The first one, an alanine at position 130, fits the density quite well, while the second one, a serine at 131, is in weak density and may be somewhat disordered. The replacements at several other positions, such as 112 Gly/Ala, 116 Gly/Ala, 122 Ser/Thr, 126 Val/Ile, and 127 Ser/Val show very good correlation with the density. However, the replacement at 129, a Lys for an Ala, has weak side chain density.

Other portions of the final electron density map of

PD-MADH based on refinement with the TV-MADH "X-ray sequence" have also been examined. In several places there are apparent differences. The observation of distinct differences between corresponding residues of the two enzymes plus the ability to model most of the 31 residue C-terminal portion of the L subunit serves as further evidence for minimal bias in the PD-MADH structure determination. Some bias clearly exists, however, since position 115 could not be inserted easily into the structure.

### The Redox Cofactor of PD-MADH

Before the TTQ cofactor model was established, efforts had been made to fit a standard PQQ model into the electron density region corresponding to the cofactor. Some difficulties were encountered in doing this. Introduction of the new TTQ model greatly improved the density fitting and solved the difficulties encountered with other cofactor models as described previously.<sup>16</sup>

The TTQ redox cofactor of MADH is located on each L subunit and is positioned in a hydrophobic cavity between three antiparallel  $\beta$ -strands of the L subunit, i.e., strands 7, 6, and 9 as shown in Figure 5. Its center of mass is buried about 5 Å below the surface of the L subunit and the two indole moieties are tilted by a dihedral angle of about 40°. The modified tryptophylquinone side chain of residue 57 is oriented so that it lies in the H-L interface channel with the two carbonyl groups pointing into the channel region. The tryptophan 107 fragment of TTQ has its phenyl portion exposed at the surface of L subunit.

The orientation of TTQ within the L subunit is particularly important for its function as the redox cofactor and its role in electron transfer. Since the quinone portion of Trp-57 points into the active site channel, it may facilitate substrate binding. The mechanism of oxidative deamination of methylamine with respect of TTQ interaction is not known at this moment. Particularly, it is not clear which carbonyl group of TTQ is responsible for substrate binding. Some proposals for the mechanism of PQQ in the oxidation of other organic species<sup>36</sup> have been made which suggested that the carbonyl group at position 5 of PQQ (Fig. 1a) is involved in substrate binding. The structurally equivalent position of TTQ should be the carbonyl group at position 6 of tryptophylquinone 57 (Fig. 1c). A difference Fourier analysis of the data from a phenylhydrazine-derivatized TV-MADH crystal was conducted which showed that the inhibitor phenylhydrazine was bound at this position.<sup>13</sup> This has recently been confirmed by crystallographic studies on TV-MADH after reaction with other hydrazines (E. Huizinga and W. G. J. Hol, unpublished results).

The presence of the phenyl portion of the indole ring of Trp-107 on the protein surface may also be of importance since the electrons from the substrate

TABLE V. Amino Acid Sequence of MADH L Subunit\*

	10	20	30
AM:	A E S A G D P R	G K W K P Q D N D V	Q S C D Y W R H C S
TV:	- - - - - V D P R	A K W N P Q D N D I	Q A C D Y W R H C S
PD:	A D A P A G T D P R	A C W V P Q D N D I	Q A C D Y
	40	50	60
AM:	I D G N I C D C S G	G S L T S C P P G T	K L A S S S W V A S
TV:	I A G N I C D C S A	G S L T S C P P G T	L V A S G S X V G S
	70	80	90
AM:	C Y N P T D K Q S Y	L I S Y R D C C G A	N V S G R C A C L N
TV:	C Y N P P D P N K Y	I T A Y R D C C G Y	N V S G R C A C L N
	100	110	120
AM:	T E G E L P V Y R P	E F G N D I I W C F	G A E D D A M T Y H
TV:	T E G E L P V Y N K	D - A N D I I X C F	G G E D - G M T Y H
PD:		E F A N D I I W C F	G A E D D A M T Y H
	130		
AM:	C T I S P I V G K A	S	
TV:	C S I S P V S G A -	-	
PD:	C T I S P I V G K A	S	

\*AM, from *Methylobacterium extorquens* AM1, 129 residues, gene sequence.<sup>11</sup> TV, from *Thiobacillus versutus*, 127 residues, "X-ray" sequence, first 6 missing; 72% identical (i.e., 94 out of a total of 131 residues) to AM.<sup>13</sup> PD, from *Parococcus denitrificans*, 46 residues: first 25 of N-terminus, chemical sequence, 56% identical (14/25) to AM and 84% identical (16/19) to TV; last 31 of C-terminus, gene sequence,<sup>12</sup> 97% identical (30/31) to AM and 65% identical (20/31) to TV.

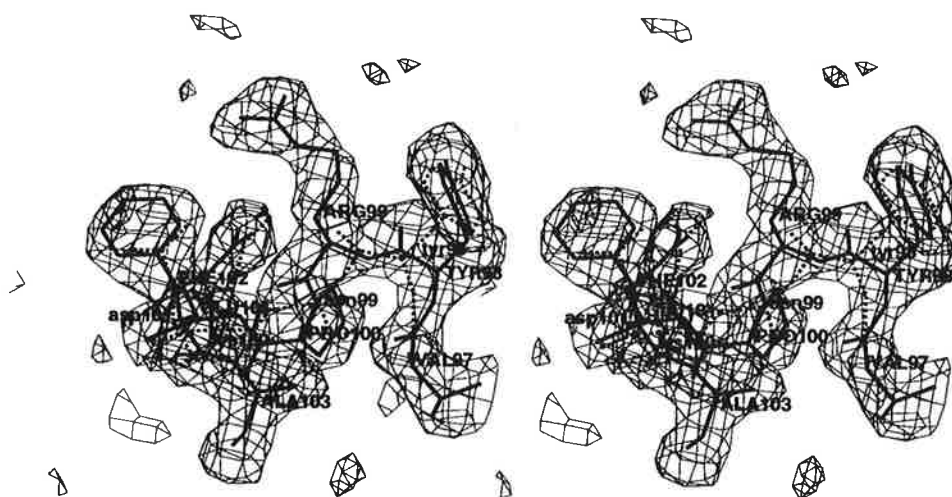


Fig. 6. The insertion at position 102 of the L subunit. The dashed model and lower case labels are the TV-MADH sequence (residues 98–101, Table V) and the solid model and upper case labels are a composite of the partial PD-MADH sequence (residues 101–103) and of the AM1-MADH sequence (residues 97–100), both compared with the PD-MADH electron density. The density is an "omit" map computed with residues 97–103 deleted from the calculated structure factors. According to the partial DNA sequence<sup>12</sup> of the L subunit of PD-MADH a phenylalanine appears to be inserted at position 102 with respect to the TV-MADH

sequence. Careful fitting of the density shows that the insertion actually occurs at position 99 where a piece of large density in the PD-MADH map was not occupied by the TV-MADH sequence. In the sequence of AM1-MADH<sup>10,11</sup> an arginine is located at position 99. Comparison of AM-MADH and TV-MADH sequences near position 99 with the PD-MADH  $F_o - F_c$  "omit" electron density shows a better fit for the former. In this figure Arg 99 is inserted into the extra density and the remaining residues are adjusted accordingly.

must eventually be transferred from TTQ to amicyanin. It has been found that in the crystal structure of the MADH–amicyanin complex, the phenyl portion of Trp-107 is located just at the interface between MADH and amicyanin and is close to the copper position of amicyanin.<sup>37</sup>

## CONCLUSION

MADH represents a newly discovered type of oxidoreductase in which the cofactor, TTQ, is derived from two gene-encoded amino acid side chains. Another oxidoreductase, mammalian serum amine oxidase, also a quinoprotein, was shown to contain

TOPA<sup>8</sup> as its redox cofactor, which is also a modified amino acid side chain. Recently, a third enzyme, galactose oxidase,<sup>38</sup> has been shown to contain a tyrosine residue which serves as a copper ligand and is also linked covalently through its side chain to a cysteine residue (Fig. 1d). This chemical grouping acts as a redox active center capable of storing 2 electrons. These three enzymes thus appear to form a novel class of redox proteins which contain cofactors directly derived from gene-encoded amino acid residues and modified posttranslationally. This class may be called amino acid-derived-cofactor oxidoreductases.

MADH and galactose oxidase have one additional unifying feature of molecular architecture in common. Each contains the rare structural motif discovered approximately 8 years ago in the influenza virus neuraminidase,<sup>39</sup> consisting of a repeating W-like  $\beta$ -leaflet arranged with circular symmetry. However, the structural and catalytic roles played by this structural element differ substantially among the three enzymes. Since complete amino acid sequences of the large subunit of both MADHs are not available, it is not yet feasible to look into a possible evolutionary convergence in the origin of these protein molecules.

The existence of TTQ as a redox cofactor in MADH presents a new set of intriguing and challenging questions about its biosynthesis. Are the cross-linking and quinolization of the tryptophan side chains catalyzed extrinsically or intrinsically, i.e., are they catalyzed by a set of different enzymes or self-catalyzed by MADH itself? Assuming that these processes involve extrinsic catalytic steps, which and how many enzymes are responsible for this side chain modification? Are they constitutive in the organism or are they induced by substrate, just as MADH is induced by methylamine? How and when does this modification occur, right after polypeptide synthesis or in the mature enzyme?

The quinolization of Trp-57 is another topic of great interest. The best-known hydroxy derivative of tryptophan in nature is 5-hydroxytryptophan, which is produced in mammals by hydroxylation of tryptophan, followed by decarboxylation which produces 5-hydroxytryptamine (5-HT, serotonin), an important neurotransmitter. Several dihydroxy derivatives of 5-HT, such as 4,5-, 5,6-, and 5,7-, all neurotoxins, occur naturally.<sup>40</sup> However, the tryptophyl quinone in TTQ is the only occurrence of a 6,7-dihydroxy derivative of tryptophan so far found in nature. Is there any relationship between the biosynthesis of 6,7- and other dihydroxy-tryptophan derivatives? These problems will present a stimulating challenge for several years to come.

#### ACKNOWLEDGMENTS

The authors express their thanks to Dr. Edwin Westbrook and Ms. Mary L. Deacon of Argonne Na-

tional Laboratory for their help during data collection. This work was supported by NSF Grant DMB-8816618 and USPHS Grant GM41574, by the Dutch Foundation of Chemical Research (SON) with financial aid from the Dutch Organization for Scientific Research (ZWO), and by the BAP Program of the EEC.

#### REFERENCES

1. Anthony, C. Methylophilic bacteria, In: "The Biochemistry of Methylophilic Bacteria." New York: Academic Press, 1982: 1-41.
2. Shirai, S., Matsumoto, T., Tobari, J. Methylamine dehydrogenase of *Pseudomonas* AM1, a subunit enzyme. *J. Biochem. (Tokyo)* 83:1599-1607, 1978.
3. Husain, M., Davidson, V.L. An inducible periplasmic blue copper protein from *Paracoccus denitrificans*: Purification, properties, and physiological role. *J. Biol. Chem.* 260: 14626-14629, 1985.
4. Husain, M., Davidson, V.L. Purification and Properties of methylamine dehydrogenase from *Paracoccus denitrificans*. *J. Bacteriol.* 169:1712-1717, 1987.
5. Ghosh, R., Quayle, J.R. Purification and properties of the methanol dehydrogenase from *Methylophilus methylotrophus*. *Biochem. J.* 199:245-250, 1981.
6. Duine, J.A., Frank, J., Jr., van Zeeland, J.K. Glucose dehydrogenase from *Acinetobacter calcoaceticus*: A quinoprotein. *FEBS Lett.* 108:443-446, 1979.
7. Ameyama, M., Matsushita, K., Ohno, Y., Shingawa, E., Adachi, O. Existence of a novel prosthetic group, PQQ, in membrane-bound, electron transport chain-linked, primary dehydrogenase of oxidative bacteria. *FEBS Lett.* 130:179-183, 1981.
8. Janes, S.M., Mu, D., Wemmer, D., Smith, A.J., Kaur, S., Maltby, D., Burlingame, A.L., Klinman, J.P. A new redox cofactor in eukaryotic enzymes: 6-Hydroxydopa at the active site of bovine serum amine oxidase. *Science* 248:981-987, 1990.
9. McIntire, W.S., Wemmer, D.E., Chistoserdov, A., Lidstrom, M.E. A new cofactor in a prokaryotic enzyme: Tryptophan tryptophylquinone as the redox prosthetic group in methylamine dehydrogenase. *Science* 252:817-824, 1991.
10. Ishii, Y., Hase, T., Fukumori, Y., Matsubara, H., Tobari, J. Amino acid sequence studies of the light subunit of methylamine dehydrogenase from *Pseudomonas* AM1: Existence of two residues binding the prosthetic group. *J. Biochem.* 93:107-119, 1983.
11. Chistoserdov, A.Y., Tsygankov, Y.D., Lidstrom, M.E. Cloning and sequencing of the structural gene for the small subunit of methylamine dehydrogenase from *Methylobacterium extorquens* AM1: Evidence for two tryptophan residues involved in the active site. *Biochem. Biophys. Res. Commun.* 172:211-216, 1990.
12. Van Spanning, R.J.M., Wansell, C.W., Reijnders, W.N.M., Oltmann, L.F., Stouthamer, A.H. Mutagenesis of the gene encoding amicyanin of *Paracoccus denitrificans* and the resultant effect on methylamine oxidation. *FEBS Lett.* 275:217-220, 1990.
13. Vellieux, F.M.D., Huitema, F., Groendijk, H., Kalk, K.H., Frank, J., Jongejans, J.A., Duine, J.A., Petratos, K., Drenth, J., Hol, W.G.J. Structure of quinoprotein methylamine dehydrogenase at 2.25 Å resolution. *EMBO J.* 8: 2171-2178, 1989.
14. Vellieux, F.M.D., Kalk, K.H., Drenth, J., Hol, W.G.J. Structure determination of quinoprotein methylamine dehydrogenase from *Thiobacillus versutus*. *Acta Crystallogr.* B46:806-823, 1990.
15. Chen, L., Lim, L.W., Mathews, F.S., Davidson, V.L., Husain, M. Preliminary X-ray crystallographic studies of methylamine dehydrogenase and methylamine dehydrogenase-amicyanin complex from *Paracoccus denitrificans*. *J. Mol. Biol.* 203:1137-1138, 1988.
16. Chen, L., Mathews, F.S., Davidson, V.L., Huizinga, E.G., Vellieux, F.M.D., Duine, J.A., Hol, W.G.J. Crystallographic investigations of the tryptophan-derived cofactor in the quinoprotein methylamine dehydrogenase. *FEBS Lett.* 287:163-166, 1991.

17. Howard, A.J. A Guide to macromolecular X-ray data reduction for the Nicolet area detector system: The XENGEN System, Version 1.3, Gaithersburg, Maryland: Genex Corporation, 1988.
18. Reeke, G.N. The ROCKS system of computer programs for macromolecular crystallography. *J. Appl. Crystallogr.* 17: 125-130, 1984.
19. Bethge, P.H. VAX adaptation of the ROCKS crystallographic program system. *J. Appl. Crystallogr.* 12:215, 1984.
20. Terwilliger, T.C., Kim, S.-H. Generalized method of determining heavy-atom positions using the difference Patterson method. *Acta Crystallogr.* A43:1-5, 1987.
21. Terwilliger, T.C., Eisenberg, D. Unbiased three-dimensional refinement of heavy atom parameters by correlation of origin-removed Patterson function. *Acta Crystallogr.* A39:813-817, 1983.
22. Wang, B.C. Resolution of phase ambiguity in macromolecular crystallography. *Methods Enzymol.* 115:90-112, 1985.
23. Rossmann, M.G., Blow, D.M. The detection of sub-units within the crystallographic asymmetric unit. *Acta Crystallogr.* 15:24-31, 1962.
24. Rossmann, M.G. Introduction. In: "The Molecular Replacement Method a Collection of Papers on the Use of Non-crystallographic Symmetry." Rossmann, M.G. (ed.). New York: Gordon and Breach, 1972: 4-15.
25. Fitzgerald, P.M.D. MERLOT, An integrated package of computer programs for the determination of crystal structures by molecular replacement. *J. Appl. Crystallogr.* 21: 273-278, 1988.
26. Crowther, R.A. Fast rotation function. In: "The Molecular Replacement Method a Collection of Papers on the Use of Non-crystallographic Symmetry." Rossmann, M.G. (ed.). New York: Gordon and Breach, 1972: 173-178.
27. Lattman, E.E. Optimal sampling of the rotation function. *Acta Crystallogr.* B28:1065-1068, 1972.
28. Crowther, R.A., Blow, D.M. A method of positioning a known molecule in an unknown crystal structure. *Acta Crystallogr.* 23:544-548, 1967.
29. Ward, K.B., Wishner, B.C., Lattman, E.E., Love, W.E. Structure of deoxyhemoglobin A crystals grown from polyethylene glycol solutions. *J. Mol. Biol.* 98:161-177, 1975.
30. Hendrickson, W.A., Konnert, J.H. Stereochemically restrained crystallographic least squares refinement of macromolecule structures. In: "Biomolecular Structure, Function, Conformation and Evolution," Vol. 1. Srinivasan, R. (ed.). Oxford: Pergamon, 1980: 43-57.
31. Brünger, A.T., Kuriyan, J., Karplus, M. Crystallographic R factor refinement by molecular dynamics. *Science* 235: 458-460, 1987.
32. Fujinaga, M., Gros, P., van Gunsteren, W.F. Testing the method of crystallographic refinement using molecular dynamics. *J. Appl. Crystallogr.* 22:1-8, 1989.
33. Finzel, B.C. Incorporation of fast Fourier transforms to speed restrained least-squares refinement of protein structures. *J. Appl. Crystallogr.* 20:53-55, 1987.
34. Bricogne, G. Methods and programs for direct-space exploitation of geometric redundancies. *Acta Crystallogr.* A32:832-847, 1976.
35. Jones, T.A. Interactive computer graphics: FRODO. *Methods Enzymol.* 115:157-171, 1982.
36. McWhirter, R.B., Klapper, M.H. Mechanism of the methylamine dehydrogenase reductive half reaction. In: "PQQ and Quinoprotein." Jongejan, J.A., Duine, J.A. (eds.). Dordrecht, the Netherlands: Kluwer, 1989: 259-268.
37. Chen, L., Durley, R., Poliks, B.J., Hamada, K., Chen Z., Mathews, F.S., Davidson V.L., Satow, Y., Huizinga, E., Vellieux, F.M.D., Hol, W.G.J. Crystal structure of an electron-transfer complex between methylamine dehydrogenase and amicyanin. *Biochemistry*, in press, 1992.
38. Ito, N., Phillips, S.E.V., Stevens, C., Ogel, Z.B., McPherson, M.J., Keen, J.N., Yadav, K.D.S., Knowles, P.F. Novel thioether bond revealed by a 1.7 Å crystal structure of Galactose oxidase. *Nature (London)* 350:87-90, 1991.
39. Varghese, J.N., Laver, W.G., Colman, P.W. Structure of the influenza virus glycoprotein antigen neuraminidase at 2.9 Å resolution. *Nature (London)* 303:35-40, 1983.
40. Dryhurst, G. Application of electrochemistry in studies of the oxidation chemistry of central nervous system indoles. *Chem. Rev.* 90:795-811, 1990.